Thermochimica Acta 518 (2011) 59–65

Contents lists available at ScienceDirect

Thermochimica Acta

journal homepage: www.elsevier.com/locate/tca

Thermal degradation and flame retardancy properties of ABS/lignin: Effects of lignin content and reactive compatibilization

Pingan Song[a], Zhenhu Cao[b], Shenyuan Fu[a,*], Zhengping Fang[b], Qian Wu[a], Jiewang Ye[a]

[a] Department of Materials, College of Engineering, Zhejiang Agriculture & Forest University, Hangzhou 311300, China
[b] Lab of Polymer Materials and Engineering, Ningbo Institute of Technology, Zhejiang University, Ningbo 315100, China

ARTICLE INFO

Article history:
Received 14 December 2010
Received in revised form 1 February 2011
Accepted 3 February 2011
Available online 22 February 2011

Keywords:
Degradation
Flammability
Lignin
ABS
Reactive compatibilization

ABSTRACT

Effects of alkali lignin incorporation and *in situ* reactive compatibilization on the thermal stability and flame retardancy of ABS were investigated. Morphology observations show that lignin can form submicron dispersed phases in ABS matrix regardless of compatibilization. Thermal analyses show that lignin will cause a slight thermal instability of ABS due to its relatively lower thermal stability, and compatibilization reaction has little effluence on that. However, lignin can slow the degradation process and increase the char residue of ABS with increasing lignin loading, and the compatibilization does not markedly affect them. Cone calorimeter tests demonstrate that lignin can significantly reduce the heat release rate, and slow the combustion process of ABS, e.g., 20 wt% lignin causing a 32% reduction in peak heat release rate (PHRR). The compatibilization can further reduce the flammability of ABS due to the improved char layer. The char residue analyses indicate that the formation of protective char layer of lignin is primarily responsible for the enhanced flame retardancy.

1. Introduction

Over the past few years, environmental concerns and realization of gradual depletion of fossil resources have driven scientists to increasingly transfer their attentions to renewable and biodegradable resources which bring no burden to the environment. Lignin, a natural non-toxic polyaromatic polyol, is one of the most abundant and relatively inexpensive sustainable polymers. Standard well-defined lignin is commercially available as a byproduct of papermaking industry [1]. It is reported that annual global production of industrial lignin reaches 50 million tons, which almost approaches the 50% of the total production of industrial plastics [2]. Owing to its abundance, low cost, and biodegradability, lignin is considered to be an extremely promising material as a chemical component in polymer blends or as organic fillers to lower the cost of the resulting products.

Recently, lignin has been employed to improve the thermal oxidation stability [3–6] and flame retardancy [7] of polymers, particularly polyolefins like polyethylene and polypropylene. The antioxidative properties of lignin are considered to be attributed to its high reactivity towards radicals which are responsible for the oxidation degradation of polymers. Since lignin is able to generate a high amount of char residue upon heating at elevated temperature in an inert atmosphere, the char-formation can reduce the combustion heat and heat release rate of polymeric materials. Lignin was reported to be a synergistic agent with other traditional flame retardants or polymer for improving the flame retardancy of polypropylene, and their combination could prolong the combustion time, enhance the char residue, reduce the heat release rate and mass loss rate during burning [7]. Moreover, Fernandes et al. [4] reported that incorporating the kraft lignin derivative could improve the thermal and photochemical stability of PVA. Compared with the PLA/ammonium polyphosphate (APP)/pentaerythritol (PER) flame retardancy composites, the materials containing equal amount of starch or lignin as carbon resource showed lower LOI values, but the V-0 rating could be achieved during UL-94 test, which was superior to that with equal amount of PER (V-2 rating) [8].

Although lignin has been used as flame retardants or flame retardancy component for polymers for many years, the flame retardancy mechanism remains to be unclear so far. Li et al. [9] recently observed the lignin above 300 °C in nitrogen atmosphere could generate a highly conjugated structure using X-ray photoelectron spectroscopy and FTIR analysis. However, lignin itself degradation process is very different from that in polymer matrix. Generally, flame retardancy effectiveness of a flame retardant strongly depends on its dispersion state in the polymer matrix and the nature of polymer matrix.

Given the above unsolved problems, we employ styrene–acrylonitrile–butadiene copolymer (ABS), an important engineering thermoplastic, as the polymer matrix, to investigate effects of lignin content and its dispersion in the matrix on the

* Corresponding author. Tel.: +86 0571 63732790; fax: +86 0571 63300311.
E-mail address: fushenyuan1963@gmail.com (S. Fu).

0040-6031/$ – see front matter © 2011 Elsevier B.V. All rights reserved.
doi:10.1016/j.tca.2011.02.007

thermal properties and flame retardancy of ABS. In addition, we also try to clarify the flame retardancy mechanism of lignin by studying the morphology and structure of char residue of samples after cone calorimeter tests.

2. Experimental

2.1. Raw materials and sample fabrication

Acrylonitrile–butadiene–styrene copolymer (ABS) was a styrene and acrylonitrile grafting modified butadiene rubber purchased from Zhenjiang Guoxiang Chemical Co., Ltd. (Hangzhou, China) with a melt flow rate of 1.7 g/10 min (200 °C, 5 kg), and its density was 1.05 g/cm^3. Lignin used in the presented work was wheat straw alkali lignin (OH%: 6.65 wt%, M_w = 6000 g/mol, polydispersity index: 5.3, Hangzhou, China), and its density was about 1.30 g/cm^3. Styrene ethylene-co-butadiene styrene-grafted-maleic anhydride (SEBS-g-MA) was produced by KRATON^{TM} Polymers (Houston, America), with a melt flow rate of 22 g/10 min (200 °C, 5 kg), maleic anhydride content of 2.0 wt%, and density of 0.91 g/cm^3, and *S*/*B* molar ratio of 30/70. Other chemicals like NaOH were used as purchased with further purification.

About 5 g lignin was purified by dissolving it in 50 ml distilled water through adjusting the pH to 10.0 using a 20 wt% aqueous solution of NaOH to enable all lignin dissolved completely, then 10 ml 10 vol.% H_2SO_4 was dropped into the aqueous solution of lignin accompanied by stirring, and followed by washing the lignin precipitation using distilled water until the washing water turned neutral. The purified lignin was dried at 80 °C under reduced pressure until the weight did not change. All ABS and its blends were fabricated via melt compounding using a ThermoHaake Torque Rheometer at 180 °C for 10 min with a rotor speed of 60 rpm for each sample. The samples were hot-pressed at 180 °C into the size required for according measurements. The identification and formulation of the blend samples were listed in Table 1.

Table 1
Sample identification and the experimental formulation of ABS/lignin blends.

Sample ID	ABS (wt%)	Lignin (wt%)	SEBS-g-MA (wt%)
ABS	100	0	0
ABS-5	95	5	0
ABS-10	90	10	0
ABS-20	80	20	0
ABSS-5	75	20	5
ABSS-10	70	20	10
ABSS-15	65	20	15
ABSS	90	0	10

2.2. Measurements and characterization

A SIRION-100 scanning electron microscope (SEM) was used to observe the micro-morphology of the fracture of samples and char residue after cone calorimeter tests at an accelerating voltage of 10 kV. The samples were coated with a 10 nm gold layer.

Thermogravimetric analysis (TGA) were performed on a TA SDTQ600 thermal analyzer at a scanning rate of 20 °C/min both in nitrogen and in air. The measurement temperature range was from room temperature to 600 °C. The TGA tests were done in triplicate for each sample. The reproducibilities of temperature and mass were ±1 °C and ± 0.1 wt%.

The flame retardancy of sample (3 mm in thickness) was evaluated using a cone calorimeter performed in an FTT UK device according to ISO 5660 with an incident flux of 35 kW/m^2. Typical results from cone calorimetry are reproducible to within around ±10% [10] and the data reported here were the means of triplicate experiments.

Raman spectra of lignin and the char residue were carried out with a ALMEGA-Dispersive Raman (Thermo Nicolet) with 514.5 nm excitation.

Infrared spectroscopy (IR) measurements were performed on a Vector-22 FT-IR spectrometer using KBr pellets for lignin and a

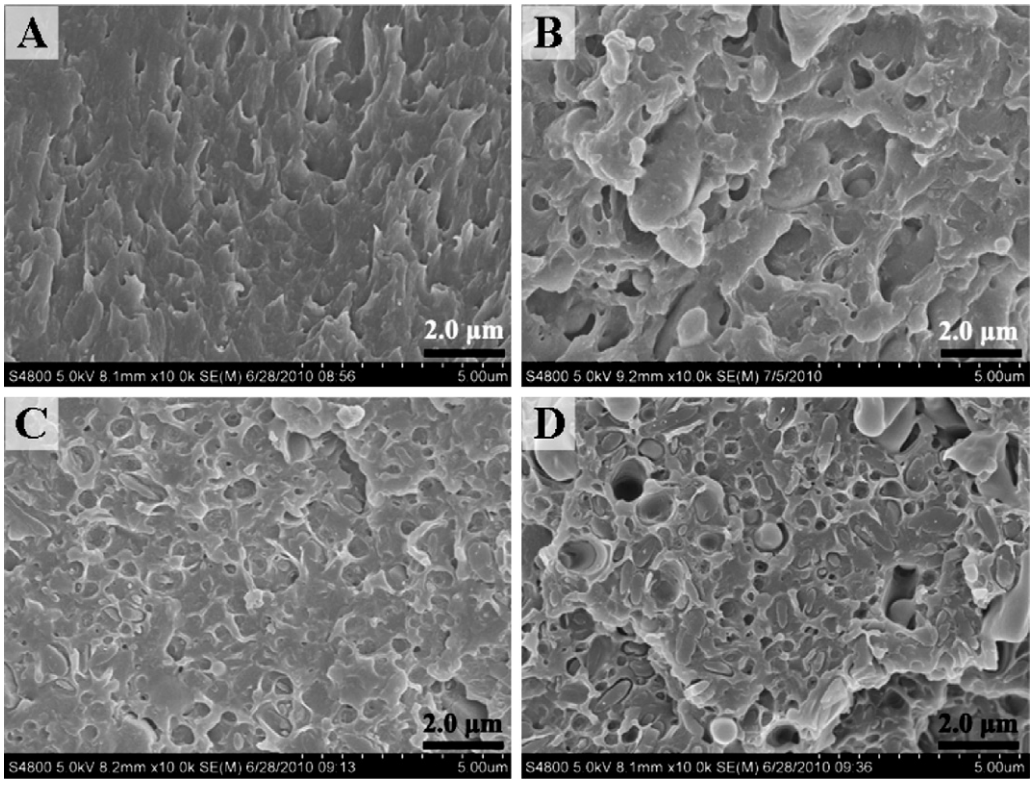

Fig. 1. SEM images of (A) ABS matrix, (B) ABSS, (C) ABS-20, and (D) ABSS-10.

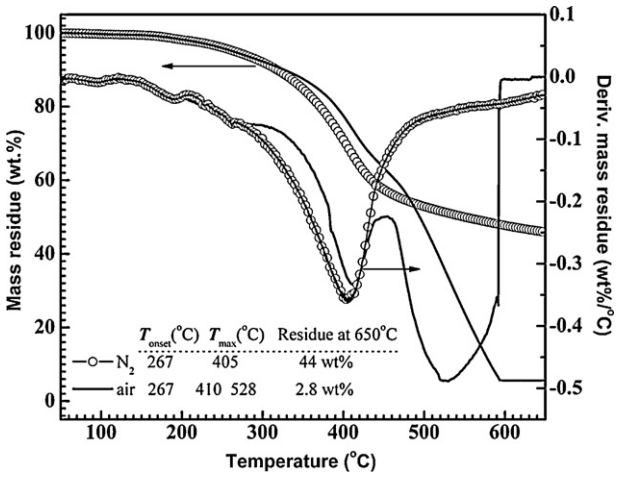

Fig. 2. Thermal analysis curves of lignin under nitrogen and air condition.

film-pressing method for ABS and its blend samples, respectively. The IR was carried out by scanning 20 times and in the range of 400–4000 cm^{-1}, with a resolution of 1 cm^{-1}.

3. Results and discussion

3.1. Dispersion of lignin in polymer matrix

Generally, the properties of particles filled composites strongly depend on the dispersion of fillers in polymer matrix. As shown in Fig. 1, ABS matrix (A) exhibits a typical micro-phase separation structure, a "sea-island" structure, in which AS phase forms the continuous ocean, while the polybutadiene rubber phase serves as the island with a domain size of 60 ± 25 nm evaluated by image analysis software. This special texture is due to the preparation methods of ABS matrix. In the case of ABSS (ABS/SEBS-g-MA, 90/10), it shows a similar morphology to ABS matrix, and the difference lies in the much bigger SEBS-g-MA phases with the size of the SEBS domains of about 1.5 ± 0.5 μm, though two components display good interfacial compatibility. For ABS/20 wt% lignin, it is readily to observe that lignin can be dispersed in the polymer matrix with a number-average domain size of ca. 250 ± 30 nm, indicating a good dispersion. After incorporating 10 wt% SEBS-g-MA as the compatibilizer, the lignin domain sizes change slightly, about 230 ± 20 nm, demonstrating a further enhanced interfacial interaction due to the compatibilization reaction between the maleic anhydride groups in SEBS-g-MA with the hydroxyl groups in lignin macromolecules.

3.2. Thermal degradation

The thermal degradation stability of lignin and its blends with ABS was studied by thermogravimetry analysis conducted under both inert and oxidative conditions. As shown in Fig. 2, lignin starts to degrade at the same temperature of 267 °C under both atmosphere, and the maximum weight loss temperature (T_{max}) takes place at 405 °C under nitrogen condition, while two-step degradation is observed for lignin under air condition with two T_{max} of 410 °C and 528 °C. As for the char residue of lignin at 650 °C, it is much more under nitrogen than under air condition, about 44 wt% and 2.8 wt%, respectively.

The TGA and DTG curves of ABS and its blends with lignin under nitrogen atmosphere are presented in Fig. 3, with detailed data listed in Table 2. ABS and its blends show a one-step degradation, the biggest difference between them is the char residue at 650 °C. Pure ABS starts to decompose at 387 °C, and T_{max} appears at 433 °C, with a char residue of 1.9 wt%. With increasing addition of lignin, both the initial degradation temperature (T_{onset}) and T_{max} gradually reduce due to lower T_{onset} and T_{max} of lignin, e.g., 353 °C (T_{onset}) and 427 °C (T_{max}) for ABS-20, while the char residue monotonously increases, e.g., 14.5 wt% for ABS-20. In addition, the maximum weight loss rate (R_{max}) gradually decreases with increasing lignin loading, which indicates that lignin enables ABS to degrade slowly, and it may be due to the protection action of char layer from the degradation of lignin at relatively low temperature. After incorporating SEBS-g-MA into ABS-20, both T_{onset} and T_{max} exhibit slight changes, and the R_{max} values decrease to some extent. Unexpectedly, the char residue to some degree reduce with increasing loading level of SEBS-g-MA, which remains to be investigated in detail in the future.

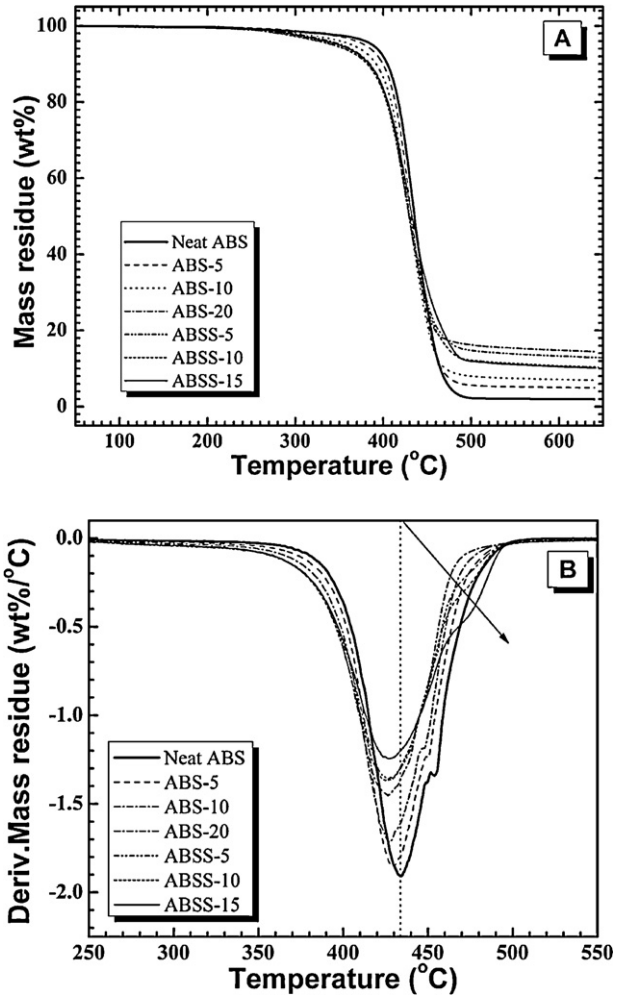

Fig. 3. (A) TGA and (B) DTG curves of ABS and its composites under nitrogen condition.

Since all polymer materials are used in air condition, it is rather necessary to investigate their thermal oxidative stability. From Fig. 4 and Table 3, we can observe that, unlike thermal degradation of ABS and its blends with lignin under nitrogen, a two-step thermal oxidative degradation takes place for them under air condition. The primary char primarily comes from the residue of lignin due to thermal degradation at elevated temperature, while the secondary char further degrades due to higher temperature and the presence of oxygen, only resulting in a small amount of char residue. Both T_{onset} and R_{max} reduce with increasing lignin loading, indicating that the addition of lignin makes ABS much easier to degrade but enabling ABS decompose slightly less slowly. On the other hand, the T_{max} and char residue increase to some extent with increasing lignin loading.

Table 2
Detailed data obtained from TGA measurements of ABS and its composites under nitrogen condition.

Run	T_{onset}[a] (°C)	T_{max}[a] (°C)	R_{max}[a] (wt%/°C)	Residue at 650 °C (wt%)
ABS	387	433	1.92	1.9
ABS-5	379	429	1.80	4.9
ABS-10	364	427	1.71	7.0
ABS-20	353	427	1.45	14.5
ABSS-5	343	427	1.35	13.0
ABSS-10	342	426	1.36	10.5
ABSS-15	350	427	1.25	10.2

[a] T_{onset} and T_{max} are the temperature where 5 wt% weight loss and maximum weight loss occurs, respectively; R_{max} refers to the maximum weight loss rate.

Table 3
Detailed data obtained from TGA measurements of ABS and its composites under air condition.

Run	T_{onset}[a] (°C)	T_{max}[a] (°C)		R_{max}[a] (wt%/°C)		Residue at 650 °C (wt%)
ABS	371	423	571	1.74	0.22	0.3
ABS-5	366	425	584	1.68	0.24	0.5
ABS-10	358	424	598	1.53	0.31	0.8
ABS-20	342	420	600	1.36	0.33	1.5
ABSS-5	333	420	574	1.35	0.39	1.4
ABSS-10	340	423	584	1.25	0.40	1.5
ABSS-15	340	423	566	1.16	0.53	1.3

[a] T_{onset} and T_{max} are the temperature where 5 wt% weight loss and maximum weight loss occurs, respectively; R_{max} refers to the maximum weight loss rate.

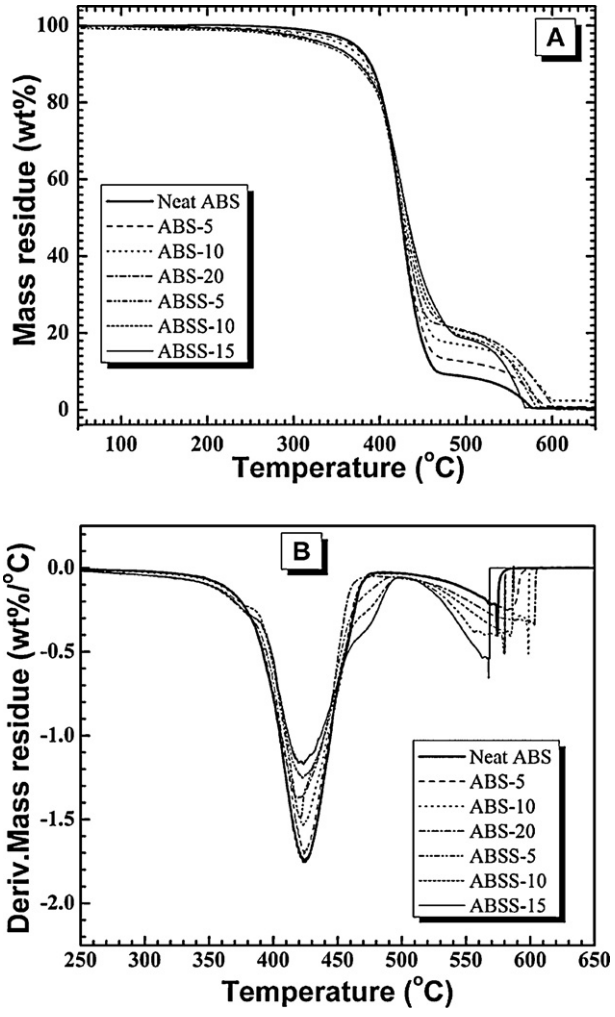

Fig. 4. (A) TGA and (B) DTG curves of ABS and its composites under air condition.

After incorporation of SEBS-g-MA, the T_{onset}, T_{max}, and char residue do not basically change, while R_{max} keeps a decreasing tendency, which suggests that lignin can confer a protective action on ABS matrix at elevated temperature.

3.3. Flame retardancy

It has been reported that incorporation of 15 wt% hydrolytic lignin can reduce the peak heat release rate (PHRR) of polypropylene by 71%, and the total combustion time is significantly prolonged during cone calorimeter tests [7]. Fig. 5 shows the heat release rate (A) and mass loss (B) as functions of combustion time, with detailed data listed in Table 4. The heat release rate curve of ABS matrix exhibits a rapid burning with a time to ignition (t_{ign}) of 24 s, a peak heat release rate (PHRR) of 775 kW/m^2, and total heat release (THR) of 71.2 MJ/m^2. With the increasing addition of lignin, the t_{ign} is first extended and then shorted at 20 wt% loading level. The PHRR and THR gradually decrease with increasing lignin loading, e.g., ABS blending with 20 wt% lignin giving a PHRR of 526 kW/m^2, a reduction by 32% relative to that of pure ABS. This reduction demonstrates that lignin incorporation can significantly improve the flame retardancy of ABS. In a previous study of our laboratory [11], incorporating 20 wt% intumescent flame retardant (PDSPB) caused a reduction by 51% relative to the pure ABS, indicating the intumescent flame retardant is more effective than lignin in terms of reducing the heat release rate. Additionally, the mass loss rate curve (Fig. 5B) shows that ABS almost combusts completely without any char residue left. The mass residue and the average mass loss rate (AMLR) monotonously increase with increasing lignin loading level. Since the char layer can act as the thermal barrier, thus the increasing char residue or low mass loss rate is responsible for the reduction in PHRR of ABS.

After compatibilization with SEBS-g-MA, the t_{ign} does not change basically, while the PHRR and AMLR reduce with increasing loading of compatibilizer, e.g., a PHRR of 428 kW/m^2 is observed for ABS/20 wt% lignin composite with 15 wt% SEBS-g-MA, a further reduction by 13% in PHRR, indicating a further enhanced flame retardancy due to the improved interfacial adhesion. In addition, the THR value reaches the minimum value upon adding 5 wt% compatibilizer, and it increases with increasing addition of compatibilizer, which may be attributed to the much easier flammability of SEBS-g-MA. These results are in good agreement with the fact that T_{onset} values lower upon adding SEBS-g-MA into ABS/lignin composites under both nitrogen and air conditions.

3.4. Flame retardancy mechanism

Though many efforts have demonstrated that lignin can undoubtedly confer some flame retardancy on many polymeric

Table 4
Cone calorimetric data for ABS/lignin composites at an incident heat flux of 35 kW/m^2.

Run	t_{ign} (s)	PHRR (kW/m^2)	PHRR reduction (%)	THR (MJ/m^2)	AMLR (g/s)
ABS	24 ± 2	775 ± 40	Non	71.2 ± 1.2	0.081 ± 0.005
ABS-5	28 ± 3	640 ± 32	18	69.1 ± 1.0	0.077 ± 0.004
ABS-10	30 ± 4	550 ± 31	29	65.4 ± 0.6	0.078 ± 0.005
ABS-20	23 ± 2	526 ± 30	32	65.1 ± 0.7	0.075 ± 0.003
ABSS-5	23 ± 2	463 ± 28	40	61.3 ± 0.5	0.074 ± 0.003
ABSS-10	24 ± 3	440 ± 30	44	63.4 ± 0.8	0.073 ± 0.004
ABSS-15	24 ± 2	428 ± 22	45	63.7 ± 0.9	0.074 ± 0.002

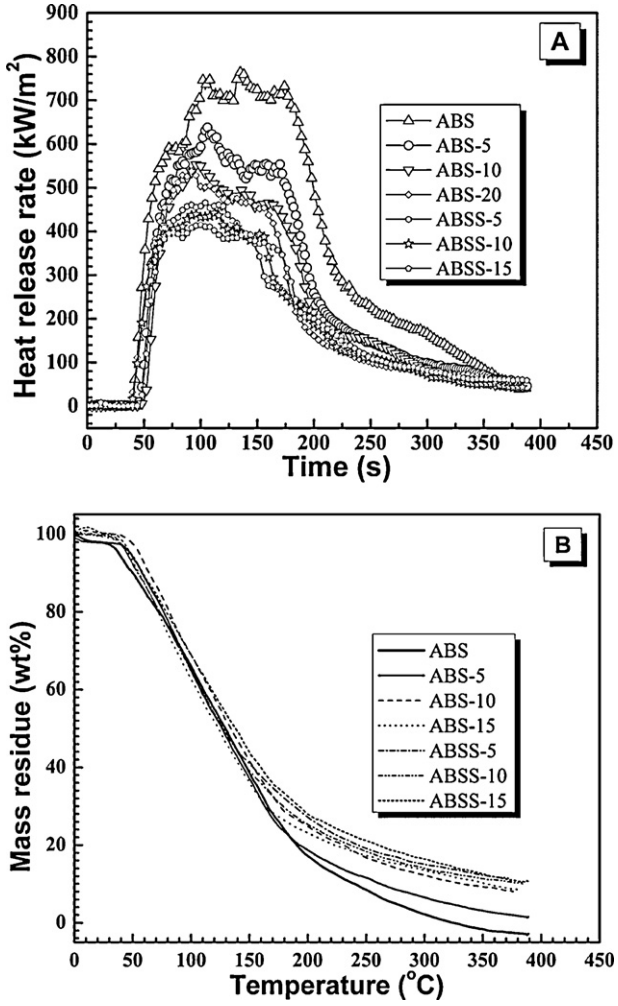

Fig. 5. (A) Heat release rate curves and (B) mass loss curves as functions of time of ABS and its composites during cone calorimeter test at an incident heat flux of 35 kW/m^2.

materials, the flame retardancy mechanism remains to be unclear. Since lignin is a polyaromatic macromolecules which will form highly conjugated structure char layer at elevated temperature, the char layer can protect the underlying polymer from degrading and further burning upon high heat flux. Moreover, the char can also provide a barrier from oxygen and small molecules from the degradation of polymers.

Fig. 6 presents the digital photographic images of char residue of ABS/lignin composites after cone calorimeter tests. Photographs of pure ABS are not showed for it leaves nothing after measurements. As shown in Fig. 6, it is not difficult to observe that the char residue steadily increases with increasing amount of lignin loading level, which can also be seen from the mass loss rate curves (see Fig. 5B). However, the char residue does not form an intact char layer, because the dispersion of lignin in the matrix is not good enough due to limited compatibility between them. Upon compatibilization, the char residue increasingly evolutes an intact or whole char layer, e.g., at 10 wt% SEBS-g-MA, the char layer almost forms a whole layer (see Fig. 6E). The improved char layer can effectively prohibits the transfer of oxygen and heat flux, and reduces the flammability of the underlying polymer. However, as the amount of SEBS-g-MA reaches 15 wt%, the char layer seems to turn poor, which suggests that too much compatibilizer will create a poor char layer, and simultaneously 10 wt% SEBS-g-MA is the optimum loading level.

Visual observations usually only provide the macroscopic understanding of char residue, thus it is necessary to further investigate the microscopic morphology and structure of char residue to deeply clarify the flame retardancy of lignin. As shown in Fig. 7, the char residue from ABS-20 presents a loose structure, namely not contact enough (see Fig. 7A and B), which in turn reflects the limited dispersion of lignin in the matrix even if the lignin domains reaches submicron size. After incorporating the compatibilizer, the char turns much compacter especially at higher magnification (see Fig. 7C and D), which can be responsible for the improved flame retardancy. Fig. 8 shows the IR spectra of lignin and char residue from ABS-20 and ABSS-10, two strong absorption bands located at ca. 3440 cm^{-1}, and 2936 cm^{-1}, 2850 cm^{-1}, are observed, which are attributed to stretching vibration of O–H and CH_2 in lignin molecules (see Fig. 8a), respectively. Peak at 1716 cm^{-1} is assigned to C=O stretching, while 1604 cm^{-1} and 1514 cm^{-1} belong to the aromatic ring vibrations [4,12]. After cone calorimeter tests, most absorption peaks almost disappear, e.g., O–H, and CH_2. Compared with ABS-20, ABSS-10 combusts more completely since both absorptions of O–H, and CH_2 completely disappear for its char, while the char of the former still leaves weak absorption peaks. Relative to the spectrum of lignin, some new peaks appear. The prominent peak locates at 1567 cm^{-1}, which should be the highly conjugated structure [9], or a polyaromatic structure, through combining another two peaks at 1120 cm^{-1} and 867 cm^{-1} which are due to the out-plane and in-plane bending vibrations of aromatic hydrogen.

To verify above IR analysis, Raman spectra are conducted, as shown in Fig. 9. Two strong peaks are observed at 1358 cm^{-1} and 1593 cm^{-1}, which belong to D band and G band, respectively, and their corresponding 2D and 2G peaks are also accompanied. Generally, the G band indicates the presence of crystalline graphitic carbon, sp^2 hybrid carbon, in the char residue, while the D band derives from the defects in the curved graphite sheet, sp^3 hybrid carbon and other impurities [13]. The appearance of these two peaks demonstrates that the char residue is a highly conjugated polyaromatic structure, as observed by Li et al. [9]. In addition, the I_G/I_D value allows us to evaluate the relative graphitic extent of the char, it is expectedly found that the I_G/I_D value of ABSS-10 char is slightly higher than that of ABS-20, which is consistent to the above IR analysis. In the case of Raman spectra of graphite [14], a very strong diffraction peak or G band appears at around 1579 cm^{-1}, and a rather weak peak or D band locates at 1353 cm^{-1}, with a high I_G/I_D value. Thus, these differences between the graphite and the

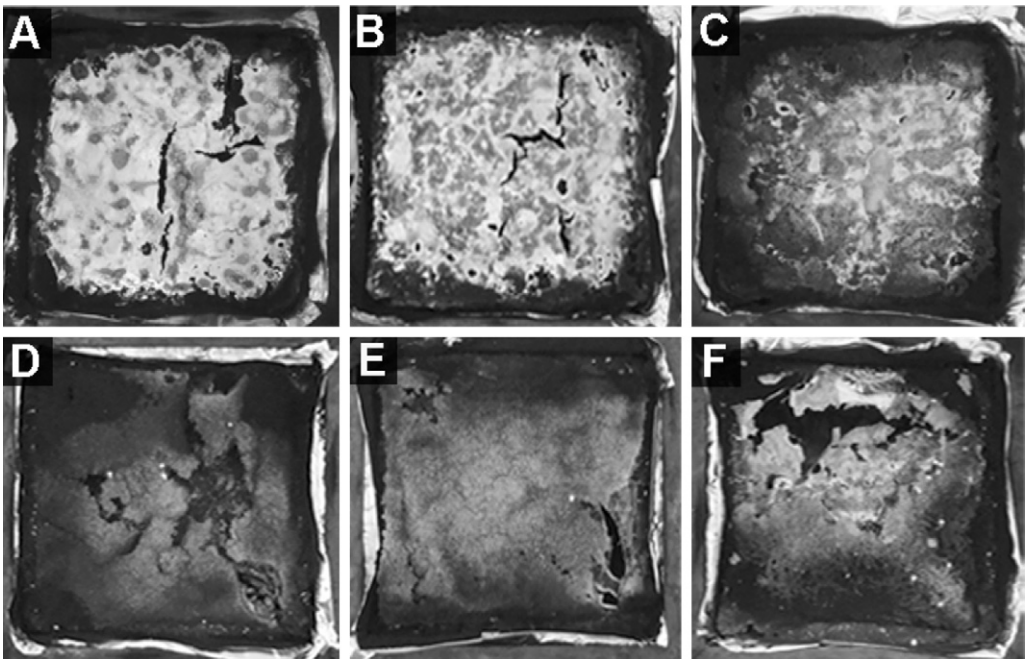

Fig. 6. Photographic images of char layers from (A) ABS-5, (B) ABS-10, (C) ABS-20, (D) ABSS-5, (E) ABSS-10, and ABSS-15 samples after cone calorimeter tests.

char from the degradation of lignin is highly defective, although the char is partially graphitic or highly conjugated polyaromatic structure.

Based on above analysis of the char residue, it is not difficult to draw the conclusion that lignin degrades at relatively lower temperature to form a highly conjugated graphitic structure, and the char can effectively reflect the heat flux and prevent the diffusion of oxygen into the underlying polymer bulk as a barrier. Moreover, it also can prohibit the degradation products transferring from the underlying heated polymer to upper combustion zone to support the burning process as fuels. In summary, the compact protective char layer is mainly responsible for the improved flame retardancy. Additionally, the radical scavenging capacity [15] of phenolic hydroxyl groups in lignin also contributes to the improved flame retardancy to some degree, and it can also be observed by the extended time to ignition at low amount of lignin (see Table 4).

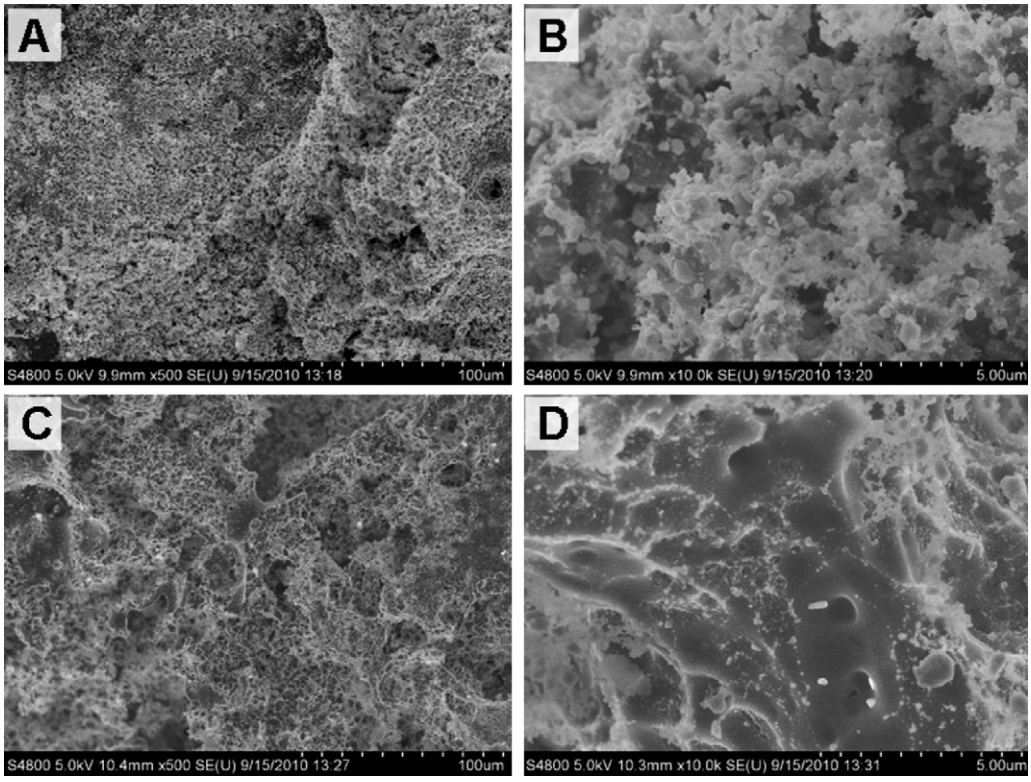

Fig. 7. SEM micrographs of char residue from (A and B) ABS-20, and (C and D) ABSS-10.

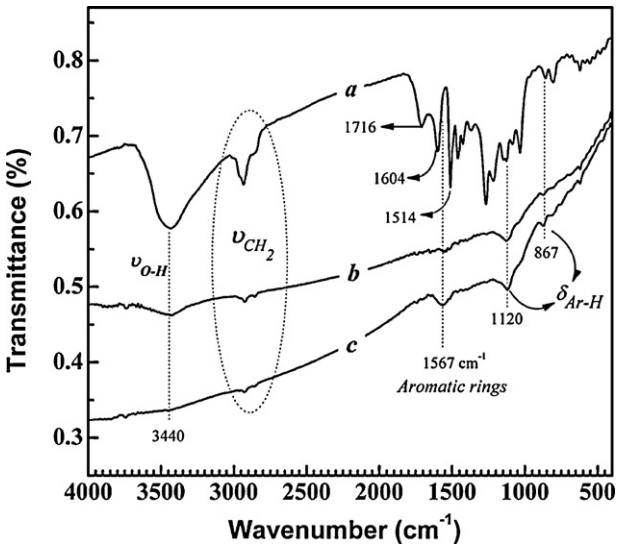

Fig. 8. Infrared spectra of (A) lignin, (B) ABS-20 char, and (C) ABSS-10 char.

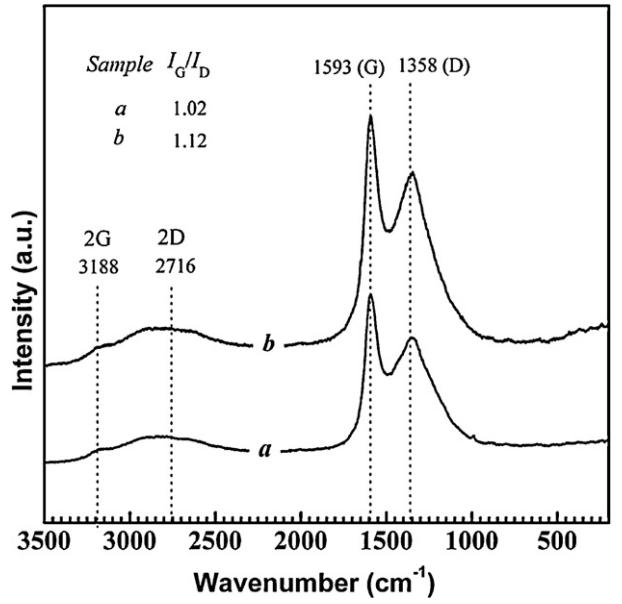

Fig. 9. Raman patterns of (A) ABS-20 char, and (B) ABSS-10 char.

4. Conclusions

The alkali lignin was blended with ABS at different loading level, and the *in situ* reactive compatibilization was also employed to improve their interfacial compatibility. The effects of lignin loading level and its dispersion on the thermal degradation stability and flame retardancy of ABS/lignin composites were studied.

The lignin can uniformly disperse in the ABS matrix, and submicron dispersed phases of lignin is achieved. Incorporating lignin will slightly reduce the initial degradation temperature of ABS under both inert and oxidative conditions due to its lower thermal stability. Lignin hardly affects the maximum loss temperature (T_{max}) of ABS under inert atmosphere, while slightly increases T_{max} under air or oxidative condition due to the radical scavenging capacity of phenolic hydroxyl groups in lignin. Addition of lignin can enhance the high-temperature stability due to the char-formation of lignin at relatively lower temperature. The compatibilization only has slight influence on the thermal stability and char formation of the composites.

Incorporating lignin can reduce the heat release rate of ABS, e.g., a 32% reduction in PHRR is observed at 20 wt% lignin loading. Total heat release (THR) and mass loss rate also decrease with increasing lignin loading. The *in situ* reactive compatibilization with SEBS-g-MA, can further reduce the flammability of ABS due to the improved char layer. As the amount of compatibilizer is 10 wt%, the PHRR reduction reaches 44% relative to pure ABS. The highly conjugated graphitic carbon layer is primarily responsible for the improved flame retardancy. Moreover, the free radical-trapping capacity of lignin also contributes to the reduced flammability of ABS.

Acknowledgements

This work was supported by Natural Science Foundation of Zhejiang Province of China (No. Y3100124 and No. Y3090190) and Scientific Research Foundation of Zhejiang Agriculture & Forestry University (No. 2351001088).

References

[1] J.C. Li, Y. He, Y. Inoue, Polym. Int. 52 (2003) 949–955.
[2] B. Xiao, X.F. Sun, R. Sun, Polym. Degrad. Stab. 71 (2001) 223–231.
[3] M. Canetti, F. Bertini, A. De Chirico, G. Audisio, Polym. Degrad. Stab. 91 (2006) 494–498.
[4] D.M. Fernandes, A.A. Winkler Hechenleitner, A.E. Job, E. Radovanocic, E.A. Gómez Pineda, Polym. Degrad. Stab. 91 (2006) 1192–1201.
[5] C. Pouteau, P. Dole, B. Cathala, L. Averous, N. Boquillon, Polym. Degrad. Stab. 81 (2003) 9–18.
[6] A. Gregová, Z. Cibulková, B. Košíková, P. Šimon, Polym. Degrad. Stab. 89 (2005) 553–558.
[7] A. De Chirico, M. Armanini, P. Chini, G. Gioccolo, F. Provasoli, G. Audisio, Polym. Degrad. Stab. 79 (2003) 139–145.
[8] C. Réti, M. Casetta, S. Duquesne, S. Bourbigot, R. Delobel, Polym. Adv. Technol. 19 (2008) 628–635.
[9] J. Li, B. Li, X.C. Zhang, R.Z. Su, Polym. Degrad. Stab. 72 (2001) 493–498.
[10] X.X. Zheng, D.D. Jiang, C.A. Wilkie, Thermochim. Acta 435 (2005) 202–208.
[11] H.Y. Ma, L.F. Tong, Z.B. Xu, Z.P. Fang, Y.M. Jin, F.Z. Lu, Polym. Degrad. Stab. 92 (2007) 720–726.
[12] J.F. Kadla, S. Kubo, Macromolecules 36 (2003) 7803–7811.
[13] W.S. Bacsa, D. Ugarte, A. Chatelain, W.A. De Heer, Phys. Rev. B 50 (1994) 15473–15476.
[14] H.F. Yang, F.H. Li, C.S. Shan, D.X. Han, Q.X. Zhang, L. Niu, A. Ivaska, J. Mater. Chem. 19 (2009) 4632–4638.
[15] A. Gregorova, B. Košíková, A. Staško, J. Appl. Polym. Sci. 106 (2007) 1626–1631.